Controllable Degradation Product Migration from Cross-Linked Biomedical Polyester-Ethers through Predetermined Alterations in Copolymer Composition

Anders Höglund, Karin Odelius, Minna Hakkarainen, and Ann-Christine Albertsson*

Department of Fibre and Polymer Technology, School of Chemical Science and Engineering, Royal Institute of Technology, S-100 44 Stockholm, Sweden

Received March 13, 2007; Revised Manuscript Received April 13, 2007

Uniformly degrading biomaterials with adjustable degradation product migration rates were customized by combining the advantages of cross-linked poly(ϵ-caprolactone) with the hydrophilic character of poly(1,5-dioxepan-2-one). Hydrolytic degradation of these random cross-linked networks using 2,2′-bis-(ϵ-caprolactone-4-yl) propane (BCP) as the cross-linking agent was studied for up to 546 days in phosphate buffer solution at pH 7.4 and 37 °C. The hydrophilicity of the materials was altered by varying the copolymer compositions. After different hydrolysis times the materials were characterized, and the degradation products were extracted from the buffer solution and analyzed. Fourier transform infrared spectroscopy, differential scanning calorimetry, atomic force microscopy, scanning electron microscopy, and gas chromatography−mass spectrometry were used to observe the changes taking place during the hydrolysis. From the results it was concluded that degradation profiles and migration of degradation products are controllable by tailoring the hydrophilicity of cross-linked polyester-ether networks.

Introduction

In the fields of tissue engineering and biomedicine, aliphatic polyesters have proven useful in a wide range of applications, such as scaffold preparation, bone fixation, sutures, and drug delivery. Polymers from ϵ-caprolactone (CL) and lactic acid (LA) are among the most extensively used materials, since they are considered biocompatible and bioresorbable and also possess favorable mechanical properties.[1,2] Aliphatic polyesters degrade in vivo by random hydrolytic scission of ester bonds. However, the hydrophobicity and crystallinity of poly(ϵ-caprolactone) (PCL) restrict the capability of water to enter the structure; hence the degradation process is slow. No significant weight loss was observed until after 80 weeks of in vivo degradation of PCL capsules with an initial molecular weight of 55 000 g/mol.[3] In a more recent study, capsules from linear PCL with an initial molecular weight of 66 000 g/mol were implanted in rats. The capsules remained intact for 24 months, with retention of their mechanical strength for 30 months.[4] Due to its slow in vivo degradation rate, PCL is most convenient for long-term drug release applications, e.g., contraceptives.

In order to increase the in vivo degradation rate and broaden its applications, PCL has been copolymerized with other degradable polyesters to reduce the crystallinity and increase the hydrophilicity. Our group has previously copolymerized CL with 1,5-dioxepan-2-one (DXO) in a variety of structures yielding materials with good elastomeric and mechanical properties.[5−7] Poly(1,5-dioxepan-2-one) (PDXO) is a hydrophilic and completely amorphous polymer with a T_g around −35 to −40 °C.[8] The reactivity factors in bulk polymerization of linear poly(DXO-co-CL) using $SnOct_2$ at 110 °C have been shown to be similar, yielding ideal random copolymers.[7] We have also previously reported on hydrolytic degradation of DXO and LA homo- and copolymers. It was concluded that degradation and formation of degradation products was dependent on copolymer composition[9] and molecular weight.[10]

Not only degradation rate but also degradation mechanism is of great importance in biomedical applications. The hydrolytic degradation is an autocatalyzed process, where the carboxylic groups of the produced hydroxy acids catalyze further hydrolysis.[3] In large size devices, there is also a risk that a substantial amount of the degradation products are released with a burst effect due to inhomogeneous degradation.[11] If an inflammatory response occurs in the vicinity of an implant of a biodegradable polyester, it is often due to the acidosis caused by the release of hydroxy acid degradation products.[12] A toxic influence was observed on cell culture systems due to high concentrations of degradation products from poly(lactic acid) (PLA).[13] Bone resorption and inflammation was induced when degradation was initiated for PLA implanted into dog femurs. Osteolytic reactions and clinically manifested foreign body reaction was the most frequent postoperative problem in a clinical study on implantation of poly(lactic acid)/poly(glycolic acid) rods.[14] It was believed that accumulation of degradation products in combination with polymer breakdown were responsible for the outcome. In another study it was suggested that cytotoxicity of PLA is due to the pH and probably the osmolarity of the tested extracts, which in turn is related to alterations in the amount of lactic acid and lactic acid oligomers.[15] It is important to consider these acidity issues when designing PCL-based biomaterials for faster degradation.

Therefore, a controllable and uniform degradation profile is an essential aspect of PCL modification. Inhomogeneous degradation can be circumvented by the utilization of networks. It has been shown that cross-linked networks of ϵ-caprolactone copolymerized with 2,2′-bis-(ϵ-caprolactone-4-yl) propane (BCP) subdermally implanted in a rabbit degraded by surface erosion with no visible bulk erosion. Onset of weight loss was observed within two weeks, and thereafter weight loss increased at an approximately linear rate to reach 80% after 107 weeks.[16] Using BCP as a cross-linking agent for CL and DXO offers an

* Corresponding author. Phone: +46-8-790 82 74. Fax: +46-8-10 07 75. E-mail: aila@polymer.kth.se.

10.1021/bm070292x CCC: $37.00
Published on Web 05/24/2007

Scheme 1. Ring-Opening Polymerization of DXO and CL with $SnOct_2$ as Catalyst in the Presence of the Cross-Linking Agent BCP

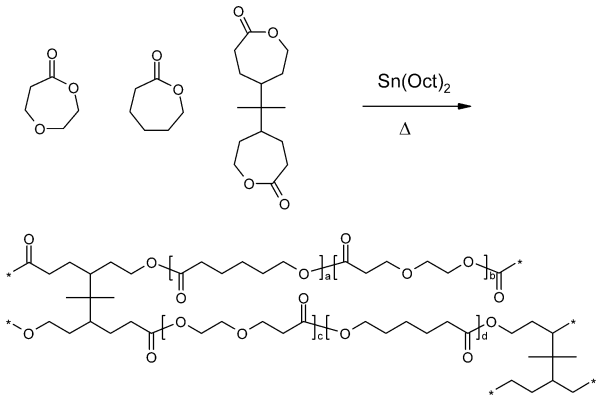

advantage by means of their resemblance in molecular structure; hence reactivity of the co-monomers is not considerably altered. Poly(ϵ-caprolactone-*co*-D,L-lactide)[17,18] and PDXO[19,20] cross-linked with BCP have also been synthesized, and their degradation has been studied.

We have reported on cross-linked networks of PCL and PDXO using BCP as a cross-linking agent.[21] The obtained networks were smooth and homogeneous with mechanical properties controlled by their cross-linking density as well as their comonomer composition. The crystallinity and hydrophilicity were customized by controlling the ratio of CL to DXO. Young's modulus and the resilient properties are improved by increasing the CL content. In a recent work, we showed that degradation rate and release of degradation products from copolymers of CL and DXO are controllable by means of macromolecular design.[22] The purpose of this study is to customize a uniformly degrading biomaterial with attuned migration of degradation products circumventing the shortcomings of materials used in short-term applications today. In order to fulfill the objective, our hypothesis was to combine and tailor the advantages of cross-linked PCL with the hydrophilic character of PDXO. A series of CL/DXO comprising materials ranging from 0 to 100% DXO with addition of 5.8% BCP were synthesized, and specimens from the materials were subjected to hydrolytic degradation in vitro for up to 546 days. The cross-link density was chosen in order to obtain a hydrophilic and elastic material with high elongation at break.[21] By scrutinizing degradation and subsequent release of degradation products, information is obtained on how to design biomedical materials with respect to degradation profiles.

Experimental Section

Materials. ϵ-Caprolactone (Aldrich, Germany) was dried and distilled over CaH_2 at reduced pressure prior to use. Stannous octoate ($SnOct_2$) (Aldrich, Germany) was distilled under reduced pressure. 1,5-Dioxepan-2-one was synthesized through a Bayer−Villiger oxidation according to the literature.[23] The DXO was then purified by recrystallization from dry ether and two subsequent distillations under reduced pressure. The monomer was dried over calcium hydride for 24 h prior to the final distillation. All monomers were stored in an inert atmosphere before use. 2,2′-Bis-(ϵ-caprolactone-4-yl) propane was synthesized according to a modified approach[21] of the procedure given elsewhere.[19] The white powder obtained was finally recrystallized from acetone and dried under vacuum.

Polymerization Technique. Networks of DXO, CL, or their mixture were created by ring-opening polymerization using BCP as cross-linking agent in the presence of $SnOct_2$ as a catalyst (Scheme 1). The monomer/monomers, cross-linking agent, and catalyst were weighed in a flask, and the mixture was dissolved in chloroform to constitute a 40 wt % solution and spread over a silanized Petri dish. The chloroform was evaporated under a nitrogen atmosphere, and the mixture was kept in an oven for cross-linking at 140 °C for an initial 1.5 h and finally at 180 °C for 30 min. The samples had a thickness of approximately 0.5 mm. The theoretical cross-linked density ρ (%) was calculated according to eq 1

$$\rho = \frac{2n}{2n + m} \times 100 \qquad (1)$$

where n is the mole fraction of BCP and m is the mole fraction of monomer/monomers in the formulation.

Hydrolysis. Cross-linked copolymer samples in the shape of polymeric discs weighting approximately 10 mg were exposed to hydrolytic degradation in a saline buffer of pH 7.4 at 37 °C. The saline buffer was prepared by dissolving 45 g of NaCl, 53.65 g of $Na_2HPO_4 \cdot 7H_2O$, and 10.6 g of NaH_2PO_4 in 4800 mL of deionized water. The solution was allowed to stand overnight whereafter the pH of the buffered solution was adjusted to 7.4 by addition of 1 M NaOH and diluted to 5000 mL with deionized water. Each specimen was placed in a vial containing 10 mL of the saline solution with the addition of 100 μL of 0.04 wt % NaN_3 solution in order to prevent microbial growth. The sample vials were sealed with septa, and they were placed in a thermostatically controlled incubator. Temperature was set to 37 °C and rotation to 60 rpm. After 1, 7, 28, 91, 182, 364, and 546 days of degradation, triplicate samples from each material were withdrawn from the test environment and subjected to the various analyses.

Solid-Phase Extraction (SPE). Hydrolysis products were extracted from the buffer medium using solid-phase extraction. A total of 2 mL of the phosphate buffer containing the degradation products were removed from each sample vial. A total of 200 μL of 1 mg/mL D,L-2-hydroxyvaleric acid sodium salt (Prosynth LTD, Suffolk, U.K.) internal standard solution was added, and pH was lowered to 1 by addition of 37% HCl. A total of 1 mL of ENV+ SPE columns (Sorbent AB, Västra Frölunda, Sweden) were used in the extractions. First, the columns were conditioned with 2 mL of methanol and equilibrated with 2 mL of acidified (pH = 1) phosphate buffer solution. The 2 mL sample portion was subsequently allowed to pass through the column, after which the retained hydrolysis products were eluted with 0.5 mL of acetonitrile. A total of 1 μL of the eluted solution was removed and analyzed with gas chromatography−mass spectroscopy.

Gas Chromatography−Mass Spectroscopy (GC-MS). The degradation products were separated and detected using a ThermoFinnigan (San José, CA) GCQ GC-MS system. A Gerstel (Mülheim an der Ruhr, Germany) MPS2 autosampler was used for injection of 1 μL of the eluted solution containing the hydrolysis products. The GC was equipped with a WCOT CP-Wax 52 CB column (30 m × 0.25 mm × 0.25 μm) from Varian (Lake Forest, CA). The column temperature was kept at 40 °C for 1 min and subsequently programmed to 250 °C at 10 °C/min, and thereafter the column was held at the elevated temperature for 13 min. The injection temperature was 250 °C, and a splitless injection mode was used. Helium of 99.9999% purity from AGA (Stockholm, Sweden) was used as carrier gas at a constant average linear velocity of 40 cm/s controlled by the electronic pressure control of the GC. The temperatures of the transfer line and the ion source were 275 °C and 180 °C, respectively. A scanning range of 35−400 m/z with a scan time of 0.43 s was used by the mass spectrometer. The peak areas were determined by integrating the total ion current using Xcalibur 1.2 software.

Fourier Transform Infrared Spectrometry (FTIR). FTIR spectra of the synthesized networks were recorded on a Perkin-Elmer Spectrum 2000 FTIR spectrometer equipped with an attenuated total reflectance accessory (golden gate) from Graseby Specac (Kent, U.K.). Specimens in the form of cut pieces from the polymer discs were placed directly on the crystal on the top-plate of the golden gate. The analysis depth

of the surface was approximately 1 μm, and all spectra were calculated means from 16 scans. The intensities of the peaks corresponding to the ether bond at 1126 cm^{-1} and the ester bond at 1185 cm^{-1} were compared in order to estimate the percentage of DXO in the polymer at the surface of the studied CL/DXO discs.

Water Absorption and Mass Loss. The degradation process was followed by determining the water absorption and mass loss of the materials. Samples were washed with distilled water and gently wiped with a tissue, and the wet weight was determined in order to evaluate the water uptake during hydrolysis. This gives an indication of the hydrophilicity of the networks. The percentage water absorption was determined by comparing the wet weight (m_w) at a specific time with the dry weight (m_d) according to eq 2.

$$\Delta m_w = \frac{m_w - m_d}{m_d} \times 100 \quad (2)$$

The percentage mass loss was determined after drying the samples for two weeks under vacuum (0.5×10^{-3} mbar) and by comparing the dry weight (m_d) at a specific time with the initial weight according to eq 3.

$$\Delta m_d = \frac{m_0 - m_d}{m_0} \times 100 \quad (3)$$

Differential Scanning Calorimetry (DSC). The thermal properties of the synthesized networks were investigated using a DSC (Mettler Toledo DSC 820 module) under nitrogen atmosphere. A total of 5−10 mg of the polymer was encapsulated in a 40 μL aluminum cap without pin. Samples were heated under a nitrogen gas flow of 50 mL/min from −65 to 80 °C at a rate of 10 °C/min. Thereafter the samples were cooled from 80 to −65 °C at a rate of 10 °C/min before being heated again from −65 to 80 °C at a rate of 10 °C/min. The melting temperatures, T_m, were noted as the maximum values of the melting peaks, and the midpoint temperature of the glass transition was determined as the glass transition temperature, T_g, from the first heating scan. When evaluating the crystallinity of the networks, it was assumed that the only contribution to the heat of fusion was from PCL. PDXO has earlier been shown to be a fully amorphous polymer having a T_g between −35 and −40 °C.[8] The approximate crystallinity of the copolymers was calculated according to eq 4

$$w_c = \frac{\Delta H_f}{\Delta H_f^\circ} \times 100 \quad (4)$$

where w_c is the degree of crystallinity, ΔH_f is the heat of fusion of the sample, and ΔH_f° is the heat of fusion of 100% crystalline polymer. The value of 139.5 J/g was used for ΔH_f°.[24]

Atomic Force Microscopy (AFM). The surface topographies were analyzed using a CSM Instrument Nano indentor with combined atomic force microscope. Samples were placed on a copper plate and aligned under the AFM tip. The measurements were performed in a dynamic contact mode in air using a Pointprobe plus probe with a nominal spring constant of ~46.5 N/m and a resonance frequency of 181−200 kHz. The length of the cantilever was 223 μm. Image analysis was performed in CSM Instruments ImagePlus v.3.1.10.

Scanning Electron Microscopy (SEM). The network samples were evaluated by means of a JEOL JSM-5400 SEM using an acceleration voltage of 15 kV. Samples were cut from the polymer discs, mounted on metal studs, and sputter-coated with gold−palladium (60%/40%) using a Denton Vacuum Desk II cold sputter etch unit operating at 45 mA for 3 × 15 s.

Results and Discussion

Networks were designed to achieve strong and elastic films with customized degradation profiles. The copolymer compositions of the cross-linked networks prior to hydrolytic degradation are shown in Table 1 and were chosen to obtain distinguished information about the effect of hydrophilicity and crystallinity on their degradation profiles. The hydrophilicity of the materials has been determined previously using contact angle measurements.[21] The results varied between 66° for CL20 to 80° for CL100 showing an increased hydrophilicity with decreasing CL content.

Table 1. Copolymer Compositions of the Cross-Linked Films Prior to Degradation

polymer name[b]	feed composition [mol %]			polymer composition[a] [mol %]		theoretical cross-linking density [%]
	DXO	CL	BCP	DXO	CL + BCP	
CL100	–	94.2	5.8	–	100	10
CL80	19.0	75.2	5.8	17.8	82.2	10
CL60	37.7	56.5	5.8	38.0	62.0	10
CL40	56.5	37.7	5.8	58.2	41.8	10
CL20	75.2	19.0	5.8	74.8	25.2	10
CL0	94.2	–	5.8	93.0	7.0	10

[a] Determined from FTIR spectra. [b] The polymer names are denotations of their monomer composition, i.e., CL80 consists of 80 % CL and 20 % DXO.

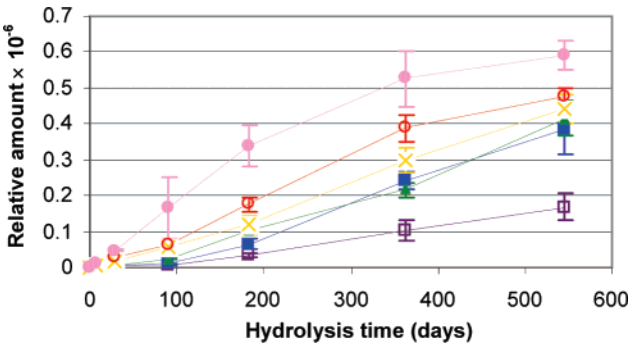

Figure 1. Relative amount of monomeric hydroxy acids migrating from (purple) CL100, (blue) CL80, (green) CL60, (yellow) CL40, (red) CL20, and (pink) CL0 during the hydrolysis.

Degradation Products. Degradation products were extracted from the buffer medium and subsequently analyzed by GC-MS. Since the degradation of polyesters in abiotic aqueous medium occurs via hydrolytic scission of the ester bonds, the expected final degradation product is the hydroxy acid corresponding to the repeating unit of the polyester. In addition, depending on the degradation mechanism and degradation state, different water-soluble oligomers are usually formed. In the case of CL/DXO copolymers, the final degradation products comprise 6-hydroxyhexanoic acid (HHA) and 3-(2-hydroxyethoxy)-propanoic acid (HPA), respectively. Figure 1 shows how the amount of monomeric acids migrating from the different cross-linked networks altered with hydrolysis time. The pH of the buffer solution was also measured after different hydrolysis times, but due to the low amount of polymer in each sample vial, no significant pH changes occurred during the aging period.

It is evident that both hydrolysis time and copolymer composition had a large influence on hydroxy acid formation. The total amount of monomeric degradation products increased at an approximately linear rate until a late stage of hydrolysis when the release rate slowed down. Higher DXO content in the copolymers resulted in a faster hydrolysis rate and hydroxy acid formation. These results are in accordance with mass loss results, which also show increasing mass loss with increasing DXO to CL ratio. Only CL100, i.e., the pure PCL network,

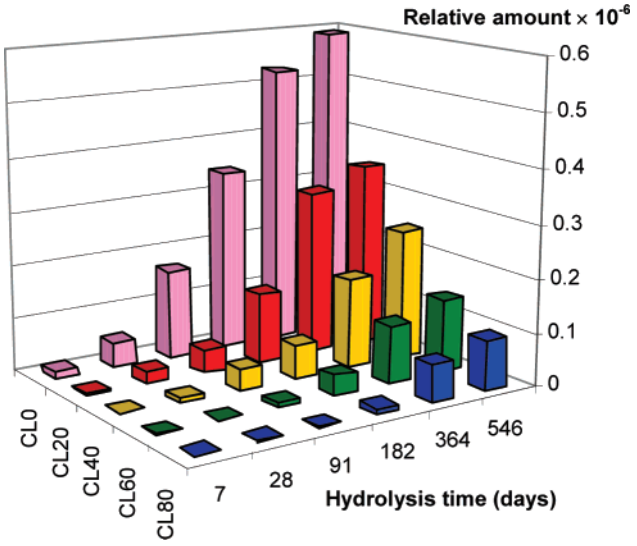

Figure 2. Relative amount of 3-(2-hydroxyethoxy)-propanoic acid (HPA) migrating from the cross-linked CL/DXO copolymers—(blue) CL80, (green) CL60, (yellow) CL40, (red) CL20, and (pink) CL0—after different hydrolysis times.

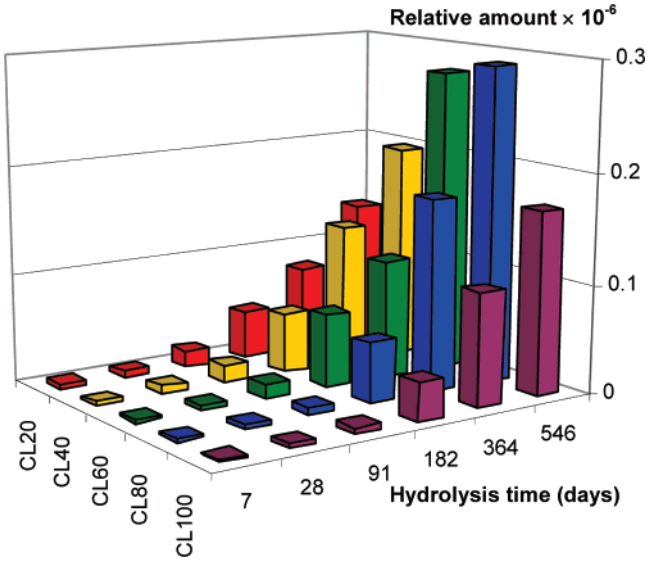

Figure 3. Relative amount of 6-hydroxyhexanoic acid (HHA) migrating from the cross-linked CL/DXO copolymers—(purple) CL100, (blue) CL80, (green) CL60, (yellow) CL40, and (red) CL20—after different hydrolysis times.

shows any remaining mass at the end of the measuring period. Nevertheless, the amount of monomeric degradation products continues to increase for all materials throughout the entire aging period. This implies that water-soluble oligomers, which were not detectable by GC-MS, continued to hydrolyze to hydroxy acids.

Figures 2 and 3 show a representation of the individual amounts of HPA and HHA respectively released to the buffer solution during degradation depending on copolymer composition and hydrolysis time.

The quantity of HPA increases with increasing DXO content in the copolymer as well as with increasing degradation time. However, the situation is a bit more complex for HHA. After 7 days, the largest amount of HHA migrated from CL20, although it had the lowest CL content of the different copolymers. At the next time point, 28 days, CL40 exhibits the highest HHA migration rate. Further, after 182 days, the largest amount of HHA migrates from CL60, and after 364 and 546 days, from

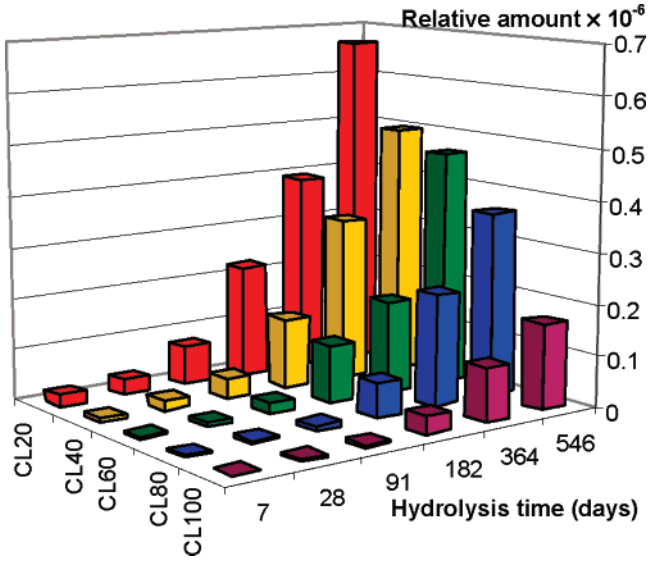

Figure 4. Amount of 6-hydroxyhexanoic acid (HHA) migrating from the cross-linked CL/DXO copolymers—(purple) CL100, (blue) CL80, (green) CL60, (yellow) CL40, and (red) CL20—in relation to the original CL content in the copolymer.

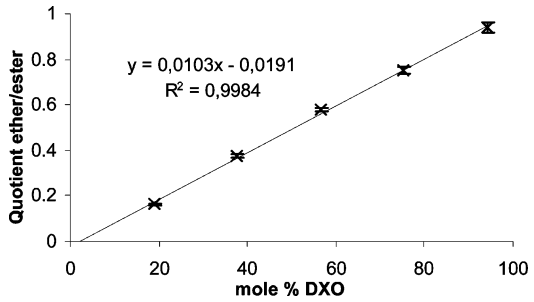

Figure 5. Quotient of the ether and ester intensities as a function of DXO content in the monomer feed determined by FTIR.

CL80. Thus, a longer degradation time is necessary for the hydrolysis of CL-units in the CL-rich copolymers to take place. This phenomenon is explained by the faster hydrolysis of DXO units, which facilitates the hydrolysis and release of HHA from the DXO-rich copolymers. The more DXO in the copolymer, the more prominent this HHA release effect becomes. On the contrary, CL degradation is delayed in copolymers with high CL to DXO ratio due to the higher hydrophobicity of the materials. The latter is endorsed by the fact that CL100 exhibits the second lowest HHA release after 546 days, although it is comprised solely of CL. In the case of CL100, crystallinity also affects the hydrolysis rate. HHA release from CL100 increased 5-fold between 91 and 182 days and 2-fold between 182 and 364 days. Linear PCL has been reported to exhibit a very low HHA release rate.[22,25−27] Much lower crystallinity for the cross-linked CL100 compared to that for the linear PCL, however, makes it less hydrolysis resistant. Hence, both cross-linking, which results in considerably lower crystallinity, and the higher susceptibility of DXO units toward hydrolysis affect the degradation rate of CL in the copolymers and accordingly the HHA migration rate.

Figure 4 shows the HHA migration in relation to the original CL content in the copolymers. The amount of HHA in relation to the amount of CL units in the copolymers not only increases with degradation time, but also with increasing DXO content in the copolymer. This trend is interestingly identical to the HPA migration, although the hydroxy acids originate from different repeating units in the copolymers. Faster hydrolysis of DXO-

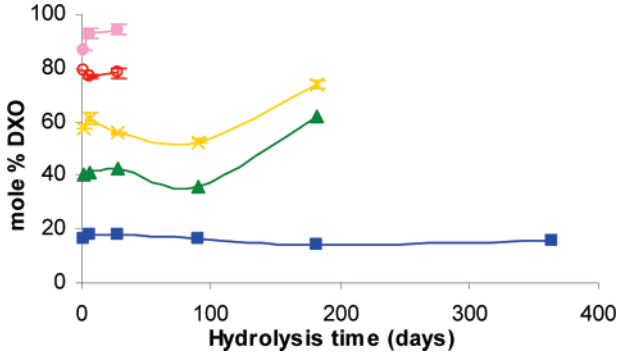

Figure 6. Content of DXO units at the surface of (blue) CL80, (green) CL60, (yellow) CL40, (red) CL20, and (pink) CL0.

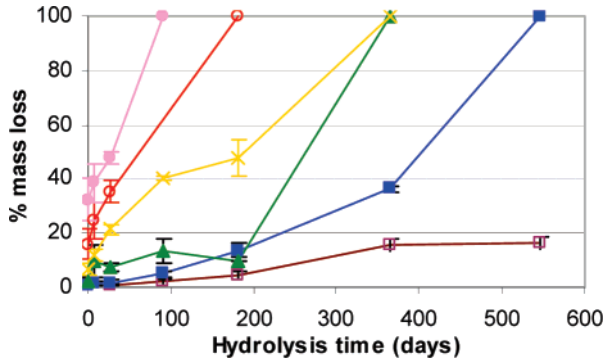

Figure 7. Mass loss profiles for (purple) CL100, (blue) CL80, (green) CL60, (yellow) CL40, (red) CL20, and (pink) CL0 after different hydrolysis times.

rich copolymers result in a high absolute HPA migration and a high relative HHA migration.

Consequently, the dependence HHA migration on the copolymer composition is two-edged. Under the prerequisite that sufficient time is given, more HHA migrates from CL-rich copolymers. However, at shorter degradation times, the highest amount of HHA migrates from copolymers with low or intermediate CL contents.

Hydrolysis-Induced Changes to the Surface Composition. The copolymer surface composition of the cross-linked networks was determined by FTIR. A calibration curve was made from calculating the quotient from the areas of the ether and ester bonds respectively for all starting materials. Triplicate measurements were made for each material. Figure 5 shows the quotient values as a function of DXO content in the feed.

The equivalent values were determined for the degraded samples, and the obtained area quotient was used to determine the surface composition of the degraded material. Figure 6 shows the content of DXO units at the surface of the materials as a function of hydrolysis time.

As expected, no ether groups were found in CL100. The surface composition of CL80 was more or less unaffected by the hydrolysis, with DXO content at just below 20%. The surface composition of CL60 and CL40 showed a small decrease in DXO content during the first 91 days. However, between 91 and 182 days both CL60 and CL40 show a considerable increase in DXO content at the surface, from 35% to 62% and from 52% to 74% respectively. The higher DXO content detected is interpreted as a migration of the formed HPA and the hydrophilic HPA-oligomers and segments toward the surface. FTIR primarily determines the copolymer composition near the surface, and hence the HPA-oligomers and HPA are detected at the surface prior to their release into the buffer solution. At early degradation states, DXO content may decrease due to the

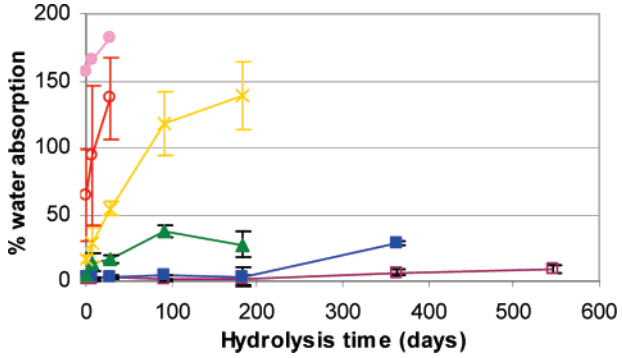

Figure 8. Water absorption profiles for (purple) CL100, (blue) CL80, (green) CL60, (yellow) CL40, (red) CL20, and (pink) CL0 after different hydrolysis times.

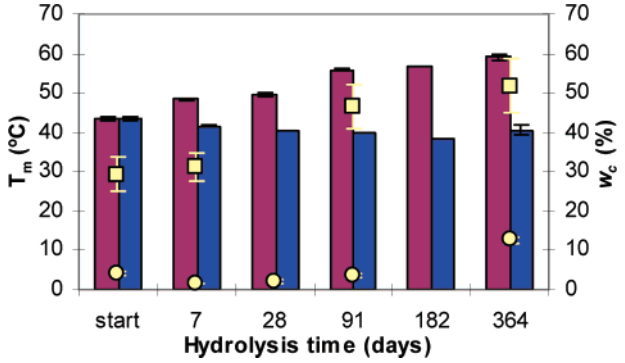

Figure 9. Influence of the hydrolysis time on the melting temperature of (purple) CL100 and (blue) CL80 and the degree of crystallinity of (yellow square) CL100 and (yellow circle) CL80 as determined from the first heating scan.

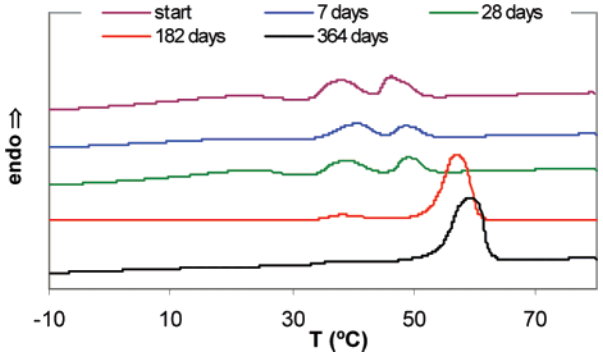

Figure 10. Changes in the thermographs for CL100 depending on hydrolysis time.

release of DXO or HPA- oligomers present at the surface prior to hydrolysis. However, as degradation proceeds, HPA and HPA-oligomers formed due to the hydrolysis of the networks migrate toward the surface. Both CL20 and CL0 possess almost constant copolymer compositions during the relatively short measuring period (28 days).

Water Absorption and Mass Loss. The hydrolytic degradation was also examined by determining the mass loss and water absorption of the samples after different hydrolysis times, Figure 7 and 8, respectively.

All networks exhibited some mass loss and water absorption, but the extent varied significantly with copolymer composition. CL100 was only moderately affected by the phosphate buffer due to its hydrophobicity, exhibiting only 16.6% mass loss and 9.5% water absorption after 546 days of degradation. In vivo studies on BCP cross-linked PCL showed around 50% mass loss during a similar aging period.[16] The generally somewhat

Table 2. Changes in the Glass Transition Temperature Determined from the First Heating Scan at Different Degradation Times

polymer name	T_g [°C] at different degradation times						
	start	1 day	7 days	28 days	91 days	182 days	364 days
CL80	−53.9 ± 0.5	−54.4 ± 0.2	−54.4 ± 0.0	−54.3 ± 0.1	−55.5 ± 0.3	−50.7 ± 0.0	−49.2 ± 0.5
CL60	−49.2 ± 0.4	−50.3 ± 0.7	−49.6 ± 0.4	−49.3 ± 0.8	−48.2 ± 0.3	−44.9 ± 0.3	–
CL40	−44.1 ± 0.9	−43.9 ± 0.5	−42.5 ± 0.1	−42.2 ± 0.2	−42.7 ± 0.5	−39.5 ± 0.3	–
CL20	−39.4 ± 0.5	−36.5 ± 0.7	−35.9 ± 0.8	−35.5 ± 0.7	−36.4 ± 1.0	−35.3 ± 1.0	–
CL0	−35.2 ± 0.5	−30.4 ± 0.6	−28.3 ± 0.9	−29.7 ± 0.5	–	–	–

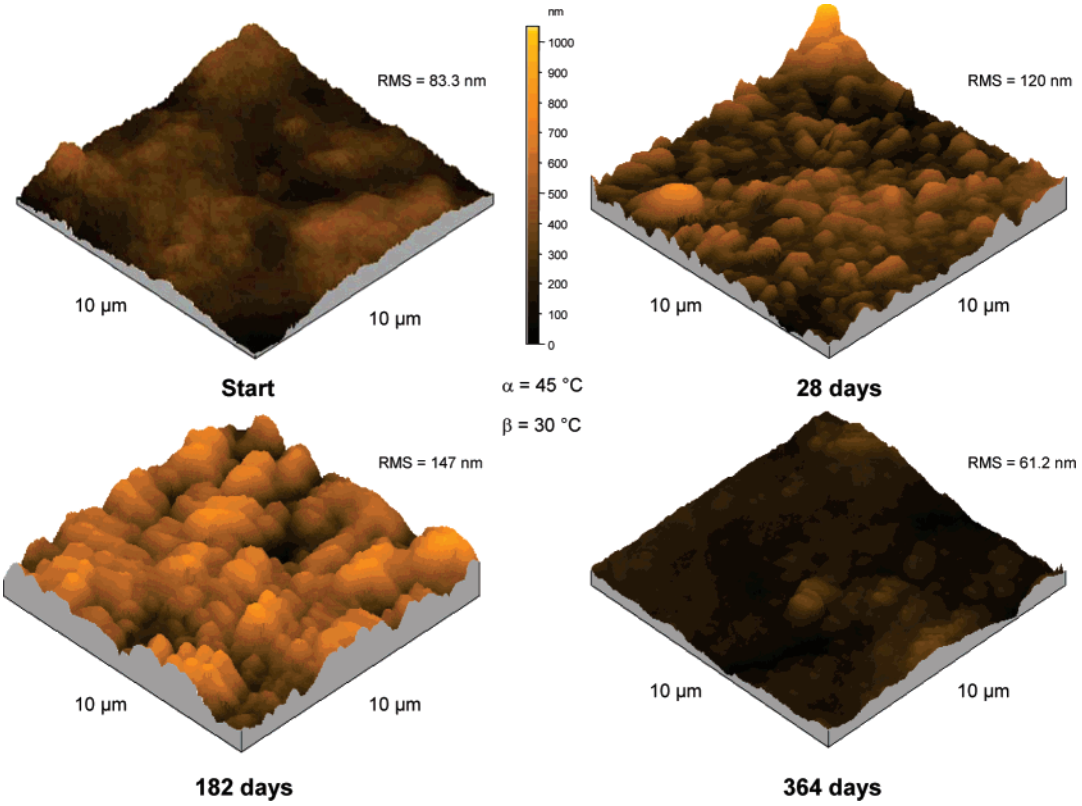

Figure 11. Changes in surface topographies during degradation of CL100 as observed by AFM.

faster degradation rate in vivo might have been further facilitated by a slightly higher cross-linking density of 12.3% which further suppresses the crystallinity of the material. In the case of linear PCL, mass loss and water absorption are generally absent or very low at the same time point.[22,27] Incorporating only 20% of DXO into the PCL structure yielded a quadrupled mass loss and water absorption after 364 days, and the material had totally disappeared after 546 days. This indicates that the slightly higher hydrophilicity together with somewhat lower crystallinity had a considerable effect on degradation rate. CL40 demonstrates a relatively rapid mass loss and water uptake at the beginning of hydrolysis, with 40% mass loss and 118% water absorption after 91 days. However, between 91 and 182 days, both mass loss and water absorption increased more slowly to 48% and 140%, respectively. After 364 days, all CL60 and CL40 had vanished. Thus, all the material had been transformed to water-soluble oligomers and hydroxy acids. The amount of monomeric hydroxy acids released from CL60 and CL40 continued to increase relatively rapidly after 182 days. This indicates further hydrolysis of oligomers to monomeric degradation products. CL20 and CL0 show similar trends with a rapidly increasing mass loss and water absorption already after short degradation times. CL0 had totally disappeared after 91 days, and CL20 was impossible to weigh at the same time point since it dissolved in the buffer immediately upon contact. We have previously reported that total degradation of PDXO cross-linked with 16% BCP was observed after 55 weeks.[20] More recent studies have shown an increased contact angle with increased cross-link density.[21] This indicates that the disparity in degradation times is probably mainly due to the increased hydrophobicity resulting from the incorporated BCP and the shaking of the samples in the present study, although other factors such as monomer and catalyst residues may also influence the degradation rate. Apparently, degradation rate decreased with increasing BCP content for PDXO whereas the opposite applies for PCL. However, a more thorough investigation is required to establish this relationship.

Thermal Properties. DSC was used to monitor the degree of crystallinity and thermal properties of the networks before and after aging. The glass transition temperature (T_g), melting point (T_m), and heat of fusion (ΔH_f) were screened during the first and second heating scan. Random linear copolymers of DXO and CL synthesized with $SnOct_2$ have been shown to crystallize when the molar fraction of DXO is 40% or lower.[7] This same trend is seen for the studied networks before degradation. However, CL100, CL80, and CL60 all have about 25−30% lower w_c than their linear analogues.[7] The cross-links restrict the chain mobility and thereby the polymers ability to crystallize, and when cross-links are incorporated by cross-

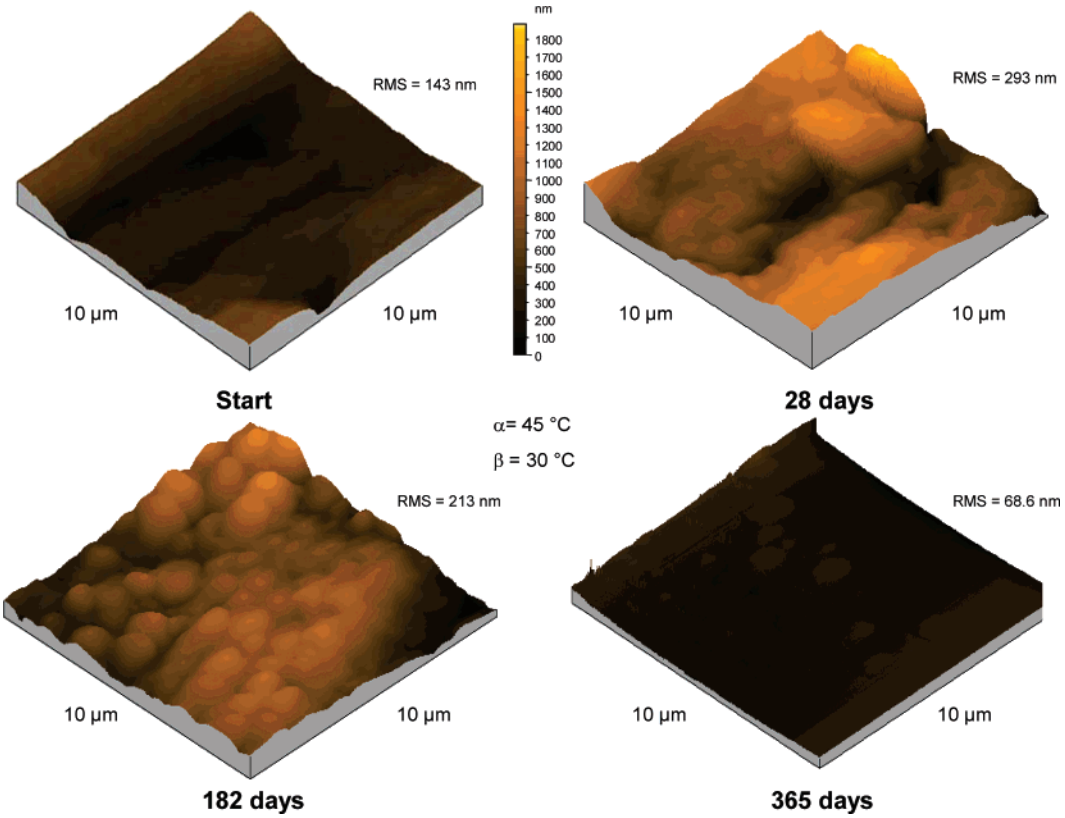

Figure 12. Changes in surface characteristics during degradation of CL80 as observed by AFM.

linking agents new units are added into the system disturbing the crystallization.

Before degradation CL100 and CL80 have similar starting T_m, indicating that the incorporation of a small amount of DXO into the networks does not lower the melting temperature to a large extent. This temperature is similar to what is found for linear polymers with 20% DXO in their main chain.[7] At early degradation stages, bimodal melting peaks were observed for CL100 and CL80. The value for T_m was taken from the first melting peak since it was larger than the second melting peak. In the second heating scan no melting peak can be seen for CL80. After 182 days of degradation CL40 and CL20 also crystallize; however, to a very low degree and only visible in the first heating scan (data not shown). For CL100, an increase in the T_m and in the w_c is observed already after 7 days, while for CL80 the degree of crystallinity is almost constant over the first 91 days after which it increases. The T_m decreases slightly with degradation time, Figure 9. This trend was also observed if the second peak of the bimodal curve at early degradation times was chosen.

The increase in w_c is due to the faster hydrolysis of amorphous regions in the materials. Prolonged aging times also allow the materials to crystallize further. In addition, as a result of chain scissions the materials may loose their network structures to some extent, which facilitates the crystallization process. In CL100, T_m may increase as a result of the formation of thicker and more perfect lamellae. The decrease in T_m observed for CL80 might be an effect from a decrease in molecular weight and thinner less perfect lamellae due to the disturbing DXO units. FTIR and GC-MS results for CL80 showed small variations in copolymer composition and release pattern of monomeric hydroxy acids, respectively. This indicates that the deviation in T_m for the two materials was not attributable to hydrolysis of DXO units. The lower T_m and w_c from the second heating scan compared to the first heating scan can be explained by the imperfect crystallization during the cooling. Figure 10 shows the changes in thermographs for CL100 during degradation. At 7 and 28 days of degradation, the curves are bimodal, but after 182 and 364 days, the first of these melting peaks has disappeared and a single melting peak is observed. This might also be a consequence of the formation of thicker lamellae during degradation; hence T_m increases and the two peaks integrate.

Table 2 shows how the glass transition temperature changes during the aging period. As expected, the cross-linked polymers had a higher T_g than their non-cross-linked analogues.[7] It is also seen that for all networks T_g increases at early degradation times, with the exception of CL0. This is an unexpected result, since the higher chain mobility obtained during degradation should result in a decrease in T_g. The finding is here explained by the increasing polarity in the networks during degradation. Hydroxy and carboxyl end-groups are formed by hydrolysis and are, due to the system's cross-linking, trapped in the networks. This yields stronger secondary interactions in the networks and hence a higher T_g. However, at later degradation stages T_g decreases due to the network disruption.

Surface Topography. AFM and SEM were used to examine the surface characteristics of the cross-linked networks. Generally, materials with a high amount of DXO possessed a smooth surface, which is in accordance with previous studies.[21] The surfaces of the DXO-rich copolymers remained smooth regardless of hydrolysis time. However, the surface topographies of the networks with lower DXO content changed during degradation.

Figure 11 shows AFM images for CL100 after different hydrolysis times. During the first 182 days of degradation the surface becomes rougher with numerous small hills. However, after 365 days the surface levels off and resembles the initial structure. This is also illustrated by the root mean square value (rms) which increases during the first 182 days and thereafter

decreases. This phenomenon is also observed for CL80; however, the dimensions of the hills are larger at short degradation times (Figure 12). In addition, the rms values are generally higher for CL80 and they start to decrease already after 28 days. After 364 days, the rms value of CL80 is approximately half of the original value and about the same as the rms value of CL100 at the same time point.

The observed elevations are interpreted as aggregations of PCL and BCP since CL100 and CL80 were the only crystalline materials. The changes in surface topography might be due to degradation of amorphous parts while the crystalline regions are preserved. The surface of the completely amorphous materials degraded more evenly and remained smooth. Smoother surfaces at early degradation states for CL100 and CL80 and throughout the measuring period for CL40−CL0 were also observed in SEM, although at a larger scale (not shown).

Conclusions

Degradation profiles and the release rate of degradation products from cross-linked films of CL and DXO with BCP as a cross-linking agent were tailored when the comonomer ratio was altered. The amount of released monomeric hydroxy acids was controllable by tuning the hydrophilicity of the biomaterial. Increasing the DXO content did not only increase the amount of released HPA but, due to the inherent properties of DXO, also affected the individual release profile of HHA. At short degradation times more HHA was released from the copolymers with larger DXO to CL ratio. If the HHA release was related to the CL content in the copolymers, then the HHA release rate increased as a function of increasing DXO content during the whole aging period. The amount of hydroxy acids detected continued to increase even after 100% mass loss, which indicates formation of water-soluble oligomers. Cross-linked networks with tailored hydrophilicity are demonstrated to be homogenously degrading biomaterials with adjustable degradation product migration rates.

Acknowledgment. The authors gratefully acknowledge The Swedish Foundation for Strategic Research (Grant A302:139) for their financial support of this work.

References and Notes

(1) Albertsson, A.-C.; Varma, I. K. *Biomacromolecules* **2003**, *4*, 1466−1486.
(2) Vert, M. *Biomacromolecules* **2005**, *6*, 538−546.
(3) Pitt, C. G.; Chasalow, F. I.; Hibionada, Y. M.; Klimas, D. M.; Schindler, A. *J. Appl. Polym. Sci.* **1981**, *26*, 3779−3787.
(4) Sun, H.; Mei, L.; Song, C.; Cui, X.; Wang, P. *Biomaterials* **2006**, *27*, 1735−1740.
(5) Loefgren, A.; Albertsson, A.-C.; Dubois, P.; Jerome, R.; Teyssie, P. *Macromolecules* **1994**, *27*, 5556−5562.
(6) Loefgren, A.; Renstad, R.; Albertsson, A.-C. *J. Appl. Polym. Sci.* **1995**, *55*, 1589−1600.
(7) Albertsson, A.-C.; Gruvegaard, M. *Polymer* **1995**, *36*, 1009−1016.
(8) Mathisen, T.; Masus, K.; Albertsson, A.-C. *Macromolecules* **1989**, *22*, 3842−3846.
(9) Karlsson, S.; Hakkarainen, M.; Albertsson, A.-C. *J. Chromatogr., A* **1994**, *688*, 251−259.
(10) Stridsberg, K.; Albertsson, A.-C. *Polymer* **2000**, *41*, 7321−7330.
(11) Li, S.; Garreau, H.; Vert, M. *J. Mater. Sci.: Mater. Med.* **1990**, *1*, 123−130.
(12) Athanasiou, K. A.; Niederauer, G. G.; Agrawal, C. M. *Biomaterials* **1996**, *17*, 93−102.
(13) Ignatius, A. A.; Claes, L. E. *Biomaterials* **1996**, *17*, 831−839.
(14) Bostman, O.; Hirvensalo, E.; Makinen, J.; Rokkanen, P. *J. Bone Joint Surg.* **1990**, *72*, 592−596.
(15) Cordewener, F. W.; van Geffen, M. F.; Joziasse, C. A. P.; Schmitz, J. P.; Bos, R. R. M.; Rozema, F. R.; Pennings, A. J. *Biomaterials* **2000**, *21*, 2433−2442.
(16) Pitt, C. G.; Hendren, R. W.; Schindler, A.; Woodward, S. C. *J. Controlled Release* **1984**, *1*, 3−14.
(17) Younes, H. M.; Bravo-Grimaldo, E.; Amsden, B. G. *Biomaterials* **2004**, *25*, 5261−5269.
(18) Amsden, B.; Wang, S.; Wyss, U. *Biomacromolecules* **2004**, *5*, 1399−1404.
(19) Palmgren, R.; Karlsson, S.; Albertsson, A.-C. *J. Polym. Sci., Part A: Polym. Chem.* **1997**, *35*, 1635−1649.
(20) Ohrlander, M.; Palmgren, R.; Wirsen, A.; Albertsson, A.-C. *J. Polym. Sci., Part A: Polym. Chem.* **1999**, *37*, 1659−1663.
(21) Andronova, N.; Srivastava, R. K.; Albertsson, A.-C. *Polymer* **2005**, *46*, 6746−6755.
(22) Hakkarainen, M.; Höglund, A.; Odelius, K.; Albertsson, A.-C. *J. Am. Chem. Soc.* **2007**, *129*, 6308−6312.
(23) Mathisen, T.; Albertsson, A. C. *Macromolecules* **1989**, *22*, 3838−3842.
(24) Crescenzi, V.; Manzini, G.; Calzolari, G.; Borri, C. *Eur. Polym. J.* **1972**, *8*, 449−463.
(25) Huang, M.-H.; Li, S.; Vert, M. *Polymer* **2004**, *45*, 8675−8681.
(26) Huang, M.-H.; Li, S.; Hutmacher, D. W.; Schantz, J.-T.; Vacanti, C. A.; Braud, C.; Vert, M. *J. Biomed. Mater. Res.* **2004**, *69A*, 417−427.
(27) Huang, M.-H.; Li, S.; Hutmacher, D. W.; Coudane, J.; Vert, M. *J. Appl. Polym. Sci.* **2006**, *102*, 1681−1687.

BM070292X